# COMBINATION OF LOW-PULSE ALS DATA AND TERRASAR-X RADAR IMAGES IN THE ESTIMATION OF PLOT-LEVEL FOREST VARIABLES

M. Holopainen [a], R. Haapanen [b], M. Karjalainen [c], M. Vastaranta [a], J. Hyyppä [c], X. Yu [c], S. Tuominen [d], H. Hyyppä [e]

[a] University of Helsinki, Department of Forest Resource Management, Finland - (markus.holopainen,mikko.vastaranta)@helsinki.fi
[b] Haapanen Forest Consulting - reija.haapanen@haapanenforestconsulting.fi
[c] Finnish Geodetic Institute - (mika.karjainen, xiaowei.yu, juha.hyyppa)@fgi.fi
[d] Finnish Forest Research Institute, Metla - sakari.tuominen@metla.fi
University of Technology, Research Institute of Modelling and Measuring for the Built Environment, Finland - hannu.hyyppa@tkk.fi

**KEY WORDS**: Forest inventory, Forest planning, Laser scanning, Radar imaging, TerraSAR-X, k-NN, Feature selection, Genetic algorithm

**ABSTRACT:**

In the present study, the objective was to compare the accuracy of low-pulse airborne laser scanning (ALS), high-resolution noninterferometric TerraSAR-X (TSX) radar data and their combined feature set in the estimation of forest variables at the plot level. The variables studied included mean volume, basal area, mean height and mean diameter. Feature selection was based on a genetic algorithm (GA). The nonparametric *k*-nearest neighbour (*k*-NN) algorithm was applied to derive the estimates. The research material consisted of 125 tree level measured circular plots located in the vicinity of Espoo, Finland. The relative RMSEs for ALS were 30.6%, 29.4%, 12.1% and 17.5% for mean volume, basal area, mean height and mean diameter, respectively. For TSX these were 47.4%, 39.3%, 20.3% and 22.4%, and for the combined feature set 29.5%, 29.0%, 12.6% and 17.0%. The accuracies of ALS-based estimations were higher in all forest variables. The best performing combined feature set obtained by GA contained 15 features, 10 of them originating from the ALS data. The combined feature set outperformed the ALS feature set only slightly. However, due to its favourable temporal resolution, satellite-borne radar imaging is a promising data source for updating large-area forest inventories performed by low-pulse ALS inventory.

## 1. INTRODUCTION

The biggest jump in forest inventory technology in recent years has been in applications based on helicopter- and airplane-based laser scanners (ALS = airborne laser scanning) operating in the near-infrared (NIR) wavelength area. Research results have shown that ALS is as accurate as traditional ocular field measurements in estimating the stand mean volume (V) at plot level with area-based inventory methods (e.g. Naesset, 1997, 2004a, 2004b; Holmgren, 2003) or via single-tree characteristics (e.g. Hyyppä & Inkinen 1999, Leckie *et al.* 2003, Popescu *et al.* 2003, Maltamo *et al.* 2004).

Area-based laser scanning is more cost-efficient, due to its sparser pulse density. Furthermore, tree-level estimation is computationally heavier; thus in large-area inventories the plot-level approach can, at least currently, be considered more feasible. On the other hand, single-tree interpretation makes it possible to understand the joint distribution of diameter and height within the stand, which facilitates the simulation and optimization needed in planning of forest operations.

ALS is carried out at relatively low altitudes, which consequently makes it relatively expensive per area unit. Other remotely sensed data will still be needed, especially when updated information is required e.g. several times per year. Of special interest are inexpensive images with favourable temporal resolution that can be utilized in multiphase sampling and change detection in addition to the ALS measurements.

A major advantage of radar images, compared with optical region satellite images, has been their ready availability (temporal resolution) under all imaging conditions. This makes radar imaging, especially the synthetic aperture radar (SAR) carried by satellites, an intriguing option in developing methods for operational inventory of forest resources.

Most commonly, the amplitude information in SAR backscattering is exploited in the estimation of forest parameters. For example, Le Toan *et al.* (1992) used an airborne multifrequency SAR system for demonstrating the capability of SAR images in forest biomass retrieval and concluded that the cross-polarization channel of the long wavelengths (L and P bands) yielded the best sensitivities. Later, promising results (with presumably enhanced estimation accuracies) were achieved, using SRTM (Shuttle Radar Topographic Mission) SAR interferometry (Kellndorfer *et al.*, 2004), interferometric coherence (Askne *et al.*, 2003), polarimetric SAR interferometry (Papathanassiou & Cloude, 2001), and fusion of SAR with airborne laser scanning (ALS) (Nelson *et al.*, 2007). The range measurements of ALS provide very accurate geometric information on forests (Hyyppä *et al.*, 2008). The main advantage of SAR, especially in the satellite-borne system, is the very frequent imaging capability in comparison to optical satellite images, aerial imagery and ALS.

SAR measurements experienced a breakthrough similar to that in the ALS method, when in the early 2000s satellite radar imagery with spatial resolutions as high as 1-3 m (single-polarization imaging) were developed. In addition to the

improved spatial resolution, the central improvements in the new SAR satellite images have been their ability to utilize interferometry and polarimetry. In combining data from several satellite types, information from different wavelength areas can be obtained. These factors should improve the estimation accuracies in forest applications, compared with previous instrument generations.

Rauste *et al.* (2008) reported that the estimation of growing stock volume is slightly more accurate with the full-polarimetric, high-resolution Advanced Land Observing Satellite (ALOS) radar images than with the earlier Japanese Earth Resources Satellite 1 (JERS-1), but the estimates still saturate at 150 $m^3$/ha. Results obtained with the RadarSat-2 or the TerraSAR-X (TSX) have not yet been published. However, in the TSX an airborne sensor, the Experimental Synthetic Aperture Radar (E-SAR), owned by the German Aerospace Centre (DLR), has been used to simulate the results obtainable with the TSX. Holopainen *et al.* (2009) compared E-SAR, Landsat Extended Thematic Mapper (ETM) and aerial photographs in estimation of plot-level forest variables and reported relative root-mean-squared-errors (RMSEs) for E-SAR of 45%, 29%, 28% and 38% for Vol ($m^3$/ha), mean diameter ($D_g$; cm) , mean height ($H_g$; m) and basal area (BA; $m^2$/ha), respectively. In combining E-SAR with aerial photographs, the relative RMSEs for the same variables were 38%, 26%, 23% and 33%. Holopainen *et al.* (2009) concluded that the potential for combination of high-resolution satellite radar images and ALS data should be investigated.

**The objective of the study** was to compare the accuracy of low-pulse ALS, high-resolution noninterferometric TSX radar data and their combined feature set in the estimation of forest variables at the plot level. One of the feature sets tested was based on automatic selection with genetic algorithms (GAs), others on expert knowledge. The estimation was carried out with the nonparametric *k*-nearest neigbour (*k*-NN) algorithm and we operated at the field plot level. The forest variables estimated included the Vol, BA, $H_g$ and $D_g$ of the growing stock.

## 2. METHODS

### 2.1 Study area and field data

The research material consisted of 125 tree level measured circular plots located in the vicinity of Espoo, Finland. Field measurement data from fixed-radius (7.98 m) field plots were collected from the study area in 2007 and 2008. The plots were located with ALS-based tree maps and the Global Positioning System (GPS). The following variables were measured of trees having a diameter-at-breast height (dbh) of over 5 cm: location, tree species and dbh. Tree heights were measured from 46 plots and the height model was then formulated. The volumes were calculated with standard Finnish models (Laasasenaho 1982). Plot-level data were obtained by summing the tree data. Stand characteristics according to the field measurements are presented in Table 1.

| | mean | min | max | stdev |
|---|---|---|---|---|
| Vol | 147.4 | 51.0 | 401.4 | 72.2 |
| Ba | 15.9 | 5.4 | 33.7 | 6.1 |
| Hg | 19.7 | 11.3 | 28.4 | 3.9 |
| Dg | 27.2 | 13.1 | 44.0 | 6.4 |

Table 1. Mean, range and standard deviation of the stand characteristics (n = 125).

### 2.2 Acquisition and processing of ALS data

The ALS data were acquired on 14 May 2006 with the Opetech3100 laser scanner. The flying altitude was 1000 m. The density of the returned pulses within the field plots was approximate 4 points/$m^2$. The ALS data were first classified into ground and nonground points. A digital terrain model (DTM) was then developed, using classified ground points and laser heights above ground (normalized height or canopy height) were calculated by subtracting the ground elevation from the laser measurements. Canopy heights close to zero were considered as ground returns and those greater than 2 m as vegetation returns. The data intermediate between them were considered as returns from ground vegetation or bushes. Only vegetation returns were used for ALS feature extraction. Several features were extracted from vegetation returns for sample plots. They included the maximum laser hit of the plot, mean, standard deviation and coefficient of variation of the canopy heights, penetration as vegetation returns versus total returns, height percentiles of the distribution of canopy heights from 10% to 100% with intervals of 10%, canopy cover percentile as proportion of laser returns below a given percentage (from 10% to 100% with 10% intervals) of total height. The features were calculated from first and last returns separately.

### 2.3 Acquisition and processing of TerraSAR-X images

The TSX is a German satellite equipped with a modern X band (wavelength of 3.1 cm) SAR system. The satellite was launched on 15 June 2007 and is capable of acquiring very-high-resolution SAR images at a spatial resolution of about 1 m in the Spotlight imaging mode (Düring *et al.*, 2008). In this study, three TSX Stripmap images were used (see Table 2). The image acquisition on 5 September 2008 was cancelled for unknown reasons.

| Date | Incidence angle (mid-range) | Polarization | Product | Weather |
|---|---|---|---|---|
| 4 Sep 2008 | 25.8º | VH+VV | Single-look complex | +13 ºC, no snow, fair |
| 5 Sep 2008 | - | - | Acquisition cancelled | |
| 3 Jan 2009 | 25.8º | VH+VV | Multilook Ground Range | -12 ºC, frost, fair |
| 8 Jan 2009 | 35.9º | HH+HV | Multilook Ground Range | -13 ºC, frost, fair |

Table 2. TSX stripmaps acquired from Nuuksio.

Processing of the TSX images was carried out at the Finnish Geodetic Institute (FGI). First, all images were converted to intensity images (squared amplitude), because in this study only the amplitude information of the backscattering was used (interferometric processing can be applied only to images with same imaging geometries). In order to extract plot-level specific forest information, the TSX images should be accurately registered with each other and with existing topographic maps. The side-looking imaging geometry of SAR causes image distortions, which can be rectified using a Digital Elevation Model (DEM) and a proper geocoding model. In this study. the PCI Geomatica software (PCI Geomatics, Richmond Hill, Ontario, Canada) and the digital elevation model (DEM) of the National Land Survey of Finland with a ground sampling distance of 25 m was used. The resulting RMS errors using 21 ground control points were 2.0 image pixels in the Easting direction and 1.3 pixels in the Northing direction. Moreover, the orthorectified images were visually compared to the digital maps and a very good agreement was observed. Therefore, we can safely assume that the geometric accuracy is good enough to extract plot level information.

To collect SAR features, circles with radii of 20 m were formed using the centre points of the field plots. The SAR feature extraction unit was larger than the field plot (radius 7.98 m). However, the field plot stand characteristics were also assumed to represent stand characteristics in the SAR feature extraction unit. The use of the 20-m radii ensured that enough TSX SAR pixels could be used to calculate the average backscattering intensity for the test plots. After calculation of the average intensity, the TSX SAR features were converted back to the amplitude scale (square root of intensity). Therefore, the used set consisted of 6 TSX features (3 images with 2 polarization channels) for each plot. Additionally, the average terrain slope and aspect values were calculated for the test stands, using the DEM. Finally, the TSX SAR features of the test plots were exported to feature selection and the plot-level forest variable estimation.

### 2.4 Genetic algorithm and feature selection

Generally, adding more features in the estimation process improves the output accuracy, but with increasing dimensionality the distinctive capacity of the data may weaken, with increasing noise. Therefore, the dimensionality of large datasets must be reduced. The usefulness of any input variable can be studied by measuring the correlation between the image features and forest attributes. In cases of large feature sets, this is extremely tedious. Furthermore, the image features are often highly correlated, and adding additional variables that are highly correlated with the other variables does not generally improve the estimation accuracy (although it is still possible). Guyon & Elisseef (2003) showed that even a useless variable may be useful when taken with others, and two useless variables can be useful together. Thus, filters that rank features based on correlation coefficients are not sufficient and subset selection algorithms or feature transformation is needed. Principal component analysis is one example of feature transformation, while e.g., stepwise regression (backward or forward selection) or GAs can be used to construct subsets of features. GAs are search algorithms that mimic natural selection and natural genetics (Goldberg 1989). Kudo & Sklansky (2000) compared several feature selection algorithms and concluded that sequential floating search methods worked best for small- and medium-scale problems, whereas for problems with a large number of dimensions (> 50), the GAs worked best.

In model construction, it is important to base the feature selection on the researcher's knowledge of the phenomenon and the variables affecting it; thus the use of stepwise selection methods is generally discouraged. However, there are situations in which the superiority of variables A and B over C and D is not clear. The relationships of recorded radiation or returned laser pulses and forest variables are not too straightforward (the exception being the canopy surface generated from laser height readings) and there are numerous potentially useful statistical/textural variables that can be extracted from the data. Therefore, the use of automated selection methods is justified to a certain extent.

The following feature sets were created:

- A: TSX features + features derived from the DEM
- B: All laser features
- A + B
- A_GA: Features selected from set A using GA
- B_GA: Features selected from set B using GA
- A + B_GA : Features selected from set A+B using GA

Feature sets A, B and A+B were used for benchmarking the results obtained with feature selection by GA.

Automatic feature selection was carried out, using a simple GA presented by Goldberg (1989), implemented in the GAlib C++ library (Wall 1996). It performed well in early feature selection studies by Haapanen & Tuominen (2008) and Holopainen *et al.* (2008). The GA process starts by generating an initial population of strings (chromosomes or genomes) that consist of separate features (genes). The strings evolve during a user-defined number of iterations (generations). The evolution includes the following operations: selecting strings for mating, using a user-defined objective criterion, letting the strings in the mating pool swap parts (crossing over), causing random noise (mutations) in the offspring (children) and passing the resulting strings into the next generation.

In the present study, the starting population consisted of 300-500 random feature combinations (genomes). The length of the genomes corresponded to the total number of features in each step, and the genomes contained a 0 or 1 at position i, denoting the absence or presence of image feature i. The number of generations was 30. The objective variable was a weighted combination of relative RMSEs of Vol, Dg and $H_g$, with total volume having a weight of 50% and Dg and Hg 25% each. Genomes that were selected for mating swapped parts with each other with a probability of 60-80%, producing children. Occasional mutations (flipping 0 to 1 or vice versa) were added to the children (probability 0.1-1%). The strings were then passed to the next generation. The overall best genome of the current iteration was always passed to the next generation, as well.

Two successive steps were taken to reduce the number of features to a reasonable minimum. Since the algorithm starts from a random pool of genomes, the process was repeated

several times at each step. Only features belonging to the best genome of the three repetitions in each step were included in the next step.

### 2.5 Estimation of plot-level forest variables

The k-NN method was used in the forest variable estimation (e.g. Kilkki & Päivinen, 1987; Tokola *et al.*, 1996; Franco-Lopez *et al.*, 2001 (Eq. 1)). A central assumption is that field plots (or stands) that are similar in reality will be similar in the space defined by remotely sensed data features, as well. The forest variables of any image pixel can then be estimated with the help of reference field plots measured in the field by calculating the averages of the nearest neighbours. In the present study, similarity was determined by the Euclidean distances in the image feature space. The nearest neighbours were weighted with inverse distances (Eq. 2).

$$\hat{y} = (\sum_{i=1}^{k} w_i y_i) / k \quad (1)$$

where

$\hat{y}$ = estimated value for variable y
$y_i$ = measured value for variable y at the i:th nearest field plot
w = weight of field plot i in the estimation

$$w_i = \frac{1}{{d_i}^2} / \sum \frac{1}{{d_i}^2} \quad (2)$$

where

$d_i$ = euclidean distance to the i:th nearest field plot (measured in the feature space)
k = number of neighbours used in the estimation

An essential parameter affecting the results obtained with the *k*-NN method is the number of neighbours, k, for which a value of 5 was set in this study. Selecting the value for k is always a compromise: a small k increases the random error of the estimates, while a large k results in averaged estimates and reduces the variation available in the original dataset.

### 2.6 Evalution of estimation accuracy

Evaluation of the estimation accuracy was carried out using cross-validation. In the process, each field plot at a time is left out of the reference dataset and the forest variable estimates are calculated using the remaining field plots. The estimates are then compared with the values observed in the field. The RMSE (Eq. 3), BIAS (Eg. 5), relative RMSE (Eq. 4) and relative BIAS (Eq. 6) were derived from the comparisons.

$$RMSE = \sqrt{\frac{\sum_{i=1}^{n} (\hat{y}_i - y_i)^2}{n}}, \quad (3)$$

$$RMSE\% = 100 * \frac{RMSE}{\bar{y}}, \quad (4)$$

$$BIAS = \frac{\sum_{i=1}^{n} (\hat{y}_i - y_i)}{n}, \quad (5)$$

$$BIAS\% = 100 * \frac{BIAS}{\bar{y}}, \quad (6)$$

where n = number of plots
$y_i$ = observed value for plot *i*
$\hat{y}_i$ = predicted value for plot i
$\bar{y}_i$ = observed mean of the variable in question.

## 3. RESULTS

The absolute and relative RMSEs and BIASes obtained, using the datasets studied, are presented in Table 3. The results show that the ALS-based features performed far better than the TSX -based features. The combined feature set improved results slightly. For example, the RMSE of Vol decreased from 30.6% to 29.5% when the ALS feature set was compared with the combined feature set. $H_g$ and $D_g$ can be estimated more accurately with all feature sets than Vol and BA. Both remote-sensing materials resulted in somewhat biased results (under estimations).

| | | VOL | BA | Hg | Dg |
|---|---|---|---|---|---|
| ALS | RMSE | 45.1 | 4.7 | 2.4 | 4.8 |
| ALS | RMSE-% | 30.6 | 29.4 | 12.1 | 17.5 |
| ALS | BIAS | -6.1 | -0.7 | -0.2 | -0.3 |
| ALS | BIAS-% | -4.1 | -4.4 | -1.0 | -1.0 |
| SAR | RMSE | 69.8 | 6.2 | 4.0 | 6.2 |
| SAR | RMSE-% | 47.4 | 39.3 | 20.3 | 22.4 |
| SAR | BIAS | -6.7 | -0.7 | -0.3 | -0.6 |
| SAR | BIAS-% | -4.5 | -4.7 | -1.3 | -2.1 |
| ALS+TSX | RMSE | 43.5 | 4.6 | 2.5 | 4.6 |
| ALS+TSX | RMSE-% | 29.5 | 29.0 | 12.6 | 17.0 |
| ALS+TSX | BIAS | -3.1 | -0.4 | -0.1 | -0.2 |
| ALS+TSX | BIAS-% | -2.1 | -2.8 | -0.6 | -0.9 |

Table 3. Accuracy of the estimated stand characteristics.

Reduced feature sets outperformed the original sets (A, B, A+B): the Vol RMSE percentages decreased by 6-7 percentage points during the GA selection process. The number of features selected by GA for the final sets were 13, 12 and 15 for the TSX (+DEM), ALS and combined set, respectively. When both the ALS- and TSX (+DEM) -based features were available, both types were included in the final set. However, the majority of the features selected were based on ALS data (10 over 15). Of the ALS-based features, the maximum heights of both first and last pulses were included, as well as percentiles of canopy height distribution (first pulse 70%, last pulse 40%, 50% and 70%), proportions of first returns below a given percentage of total height (CCP%, first pulse 10% and 40% and last pulse 10%) and penetration of the last pulse.

Plot-by-plot comparison of Vol estimation errors by means of TSX features and ALS-based features is shown in Figures 1 and 2. It can be seen that TSX systematically overestimates the

smallest volumes and underestimates the largest volumes. Laser-based features performed better at the upper end of the volume range.

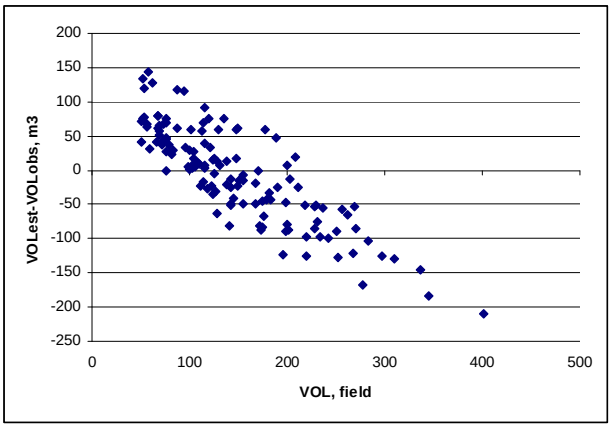


Figure 1. Volume estimation errors ($Vol_{Est}$-$Vol_{Obs}$) with best performing TSX data set.

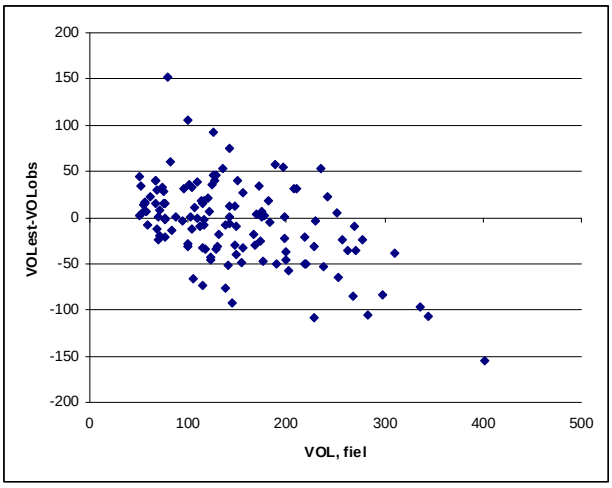


Figure 2. Volume estimation errors ($Vol_{Est}$-$Vol_{Obs}$) with best performing ALS data set.

## 4. CONCLUSIONS

In the present study, we tested the estimation of some important forest attributes in forest management planning with a combination of low-pulse ALS and TSX data, using GA feature selection and the nonparametric *k*-NN algorithm. Based on our results, the lowest RMSEs were obtained with relatively small subsets of the original features.

Our final RMSE for Vol was 29.5% of the mean. TSX features, when used separately from ALS features, gave significantly lower accuracies, i.e. the ALS data were superior to the TSX data. However, some TSX features were selected for the best-performing combined feature set. ALS and TSX RMSEs tended to be lower than with Landsat-type satellite images, which usually result in field plot-level RMSEs of 60% or greater (Tokola *et al.* 2007, Haapanen & Tuominen 2008, Holopainen *et al.* 2009).

The ALS accuracies were in line with other Finnish studies operating with low-pulse density data (e.g. Maltamo *et al.* 2006; Holopainen *et al.* 2008), but with slightly poorer results. This was probably resulted from the small number of study plots in *k*-NN estimation and smaller Vol of the stands compared with earlier studies.

In comparing our TSX accuracy to the E-SAR accuracies achieved by Holopainen *et al.* (2009), plot-level volume and BA estimations were poorer with TSX. However, the $H_g$ and $D_g$ estimations were slightly better.

The mean errors of traditional ocular forest inventory used in operational forest management planning vary from 16% to 38% in Finland (Poso, 1983; Haara & Korhonen, 2004; Saari & Kangas, 2005). This means that the approx. 30% error level reached with the combined dataset at the field plot level closely resembles that of ocular field inventory (the ALS and TSX RMSEs are probably somewhat lower at the stand level).

A central task for future forest resource inventories will be detection of changes, i.e. updating the forest inventory data. In addition to the traditional forest variables, more interest will be placed on changes in biomass, bioenergy and carbon balance. Climate change will probably increase forest damage, creating a demand for monitoring methods as well.

Our results suggest that SAR images cannot compete with ALS in large-scale precision forestry. The combined feature set only slightly outperformed ALS feature set. This is similar result to the results achieved by Nelson *et al.* (2007), who concluded that ALS is a better choice over SAR in forest biomass estimation and SAR only slightly increased the overall accuracy when ALS and SAR were used jointly in the estimation.

The exploitation of SAR images is still challenging at the moment due to the high costs, somewhat troublesome processing and tricky imaging geometries. However, we believe that high-resolution satellite SAR images may play a significant future role in nationwide forest-mapping applications, due to its higher temporal repeatability in comparison to ALS data acquisition. One promising alternative may be the use of SAR images for updating forest inventories performed by low-pulse ALS inventory.

## 5. REFERENCES

Askne, J., Santoro, M., Smith, G. and Fransson, J.E.S., 2003. Multitemporal Repeat-Pass SAR Interferometry of Boreal Forests. *IEEE Transactions on Geoscience and Remote Sensing*, 43, 6, pp. 1219-1228.

Düring, R., Koudogbo, F.N. and Weber, M., 2008. TerraSAR-X and TanDEM-X Revolution in Spaceborne Radar. *Proceedings of the ISPRS XXI Congress*, Beijing, China.

Franco-Lopez, H., Ek, A.R. and Bauer, M.E., 2001. Estimation and mapping of forest density, volume and cover type using the k-nearest neighbors method. *Remote Sensing of Environment* 77, pp. 251 - 274.

Goldberg, D.E., 1989. *Genetic algorithms in search, optimization, and machine learning.* Addison-Wesley Publishing Company, Reading, Massachusetts, 412 p.

Guyon, I. and Elisseeff, A., 2003. An introduction to variable and feature selection. *Journal of Machine Learning Research*, 3, pp. 1157-1182.

Haapanen, R. and Tuominen, S., 2008, Data combination and feature selection for multi source forest inventory. *Photogrammetric Engineering and Remote Sensing*, 74, pp. 869-880.

Haara, A. and Korhonen, K., 2004. Kuvioittaisen arvioinnin luotettavuus. *Metsätieteen aikakauskirja*, 2004, pp. 489-508.

Holopainen, M., Haapanen, R., Tuominen, S. and Viitala, R. 2008. Performance of airborne laser scanning- and aerial photograph-based statistical and textural features in forest variable estimation. In Hill, R., Rossette, J. and Suárez, J. *Silvilaser 2008 proceedings*, pp. 105-112.

Holopainen, M., Tuominen, S., Karjalainen, M., Hyyppä, J., Vastaranta, M. and Hyyppä, H. 2009. The accuracy of high resolution radar images in the estimation of plot level forest variables. *Lecture Notes in Geoinformation and Cartography*. Springer. In press.

Hyyppä, J. and Inkinen, M., 1999. Detecting and estimating attributes for single trees using laser scanner. *The Photogrammetric Journal of Finland*, 16, pp. 27-42

Kudo, M. and Sklansky, J., 2000. Comparison of algorithms that select features for pattern classifiers. *Pattern Recognition*, 33, pp. 25-41.

Kellndorfer, J., Walker, W., Pierce, L., Dobson, C., Fites, J.A., Hunsaker, C., Vona, J. and Clutter, M., 2004. Vegetation height estimation from Shuttle Radar Topography Mission and National Elevation Datasets. *Remote Sensing of Environment* 93, 3, pp. 339-358.

Laasasenaho, J. 1982. Taper curve and volume functions for pine, spruce and birch. *Communicationes Institute Forestalis Fenniae* 108. 74 p.

Le Toan, T., Beaudoin, A., Riom, J. and Guyon, D., 1992. Relating Forest Biomass to SAR Data. *IEEE Transactions On Geoscience And Remote Sensing*, 30,2, pp. 403-411.

Leckie, D., Gougeon, F., Hill, D.,Quinn, R., Armstrong, L. and Shreenan, R., 2003. Combined high-density lidar and multispectral imagery for individual tree crown analysis. *Canadian Journal of Remote Sensing*, 29, pp. 633–649.

Maltamo, M., Eerikäinen, K., Pitkänen, J., Hyyppä, J. and Vehmas, M., 2004. Estimation of timber volume and stem density based on scanning laser altimetry and expected tree size distribution functions. *Remote Sensing of Environment*, 90, pp. 319-330.

Maltamo, M., Malinen, J., Packalén, P., Suvanto, A. and Kangas, J., 2006, Non-parametric estimation of stem volume using laser scanning, aerial photography and stand register data. *Canadian Journal of Forest Research*, 36, pp. 426-436.

Næsset, E., 1997. Estimating timber volume of forest stands using airborne laser scanner data. *Remote Sensing of Environment*, 51, pp. 246-253.

Næsset, E., 2004a. Practical large-scale forest stand inventory using a small footprint airborne scanning laser. *Scandinavian Journal of Forest Research*, 19, pp. 164-179.

Næsset, E., 2004b. Accuracy of forest inventory using airborne laser-scanning: Evaluating the first Nordic full-scale operational project. *Scandinavian Journal of Forest Research*, 19, pp. 554-557.

Nelson, R.F., Hyde, P., Johnson, P., Emessiene, B., Imhoff, M.L., Campbell, R. and Edwards, W., 2007. Investigating RaDAR-LiDAR synergy in a North Carolina pine forest, *Remote Sensing of Environment*, 110, 1, pp. 98-108.

Papathanassiou, K.P. and Cloude, S.R., 2001. Single-baseline polarimetric SAR interferometry. *IEEE Transactions On Geoscience And Remote Sensing*, 39, 11, pp. 2352-2363.

Popescu, S., Wynne, R. and Nelson, R., 2003, Measuring individual tree crown diameter with lidar and assessing its influence on estimating forest volume and biomass. *Canadian Journal of Forest Research*, 29, pp. 564–577.

Poso, S., 1983. Kuvioittaisen arvioimismenetelmän perusteita. *Silva Fennica*, 17, pp. 313-343.

Rauste, Y., Lönnqvist, A., Molinier, M., Ahola, H. and Häme, T., 2008. ALOS Palsar Data in Boreal Forest Monitoring and Biomass Mapping, *Proceedings of 1st Joint PI Symposium of ALOS Data Nodes*, Kyoto, Japan, 19 - 23 Nov. 2007.

Saari, A. & Kangas, A., 2005. Kuvioittaisen arvioinnin harhan muodostuminen. *Metsätieteen aikakauskirja*, 2005, pp.5-18.

Tokola, T., Letoan, T., Poncet, F., V., Tuominen, S. and Holopainen, M. 2007. Forest Reconnaissance Surveys: Comparison of estimates based on simulated TerraSar, and optical data. *The Photogrammetric Journal of Finland*, 20, pp.64-79.

Wall, M., 1996. *GAlib: A C++ Library of Genetic Algorithm Components Version 2.4 Documentation, revision B.* Massachusetts Institute of Technology. 101 p.

## ACKNOWLEDGEMENTS

This study was made possible by financial aid from the Finnish Academy project Improving the Forest Supply Chain by means of Advanced Laser Measurements. The TerraSAR-X SAR images were acquired through the German Aerospace Center (DLR) prelaunch Announcement of Opportunity scientific project LAN-0049.